Biochemistry

 Volume 20, Number 12 June 9, 1981

Apparent Hydrogen Bonding by Strongly Immobilized Spin-Labels†

Michael E. Johnson

ABSTRACT: The hyperfine separations of nitroxide spin-labels which are tightly bound within hemoglobin exhibit a substantial temperature dependence even when the hemoglobin is immobilized by freezing or precipitation. It is shown that NO·–HX hydrogen bond formation by the spin-label within its binding site is a good explanation for the observed temperature dependence. Comparative studies using different hemoglobin derivatives and two different spin-labels suggest that the HX group may be some element of the protein matrix and that this hydrogen bond may be a factor in the stabilization of the label within its binding site. The hyperfine separation of a fatty acid spin probe incorporated into aqueous bilayer dispersions of dipalmitoylphosphatidylcholine also exhibits a temperature dependence at low temperature which is qualitatively similar to that of the spin-labeled hemoglobin systems. Saturation transfer electron paramagnetic resonance measurements indicate that label motion is not the source of this temperature dependence. A hydrogen-bond equilibrium between water molecules and the nitroxide NO· group appears to be a plausible source of the temperature-dependent hyperfine separation in the lipid bilayer system. Small amplitude torsional oscillation or librational motion by the nitroxide may also produce additional changes in the hyperfine separation which are difficult to distinguish from hydrogen-bonding effects under some circumstances. The apparent hydrogen-bond equilibrium exhibits a strong thermal and environmental dependence which may be of importance in a number of biophysical spin-label measurements.

The sensitivity of spin-label spectra to the polarity of the label environment has long been known. In the first reported application of spin-label techniques to biomolecular studies, Stone et al. (1965) reported that the rate of nitroxide rotational motion was the primary determinant of spin-label spectral shape but that polar interactions produced significant secondary effects upon both the hyperfine tensor, A, and the g tensor. The apparent mechanism of these effects is that polar interactions stabilize a negative charge on the oxygen of the NO· group and increase the spin density on the nitrogen atom.

In addition to exhibiting general sensitivity to environmental polarity, nitroxide free radicals are also Lewis bases and will form complexes with a number of electron donor reagents (Brown et al., 1971; Lim & Drago, 1971; Murata & Mataga, 1971; Kabankin et al., 1973; Cohen & Hoffman, 1973; Morishima et al., 1973; Lozos & Hoffman, 1974; Griffith et al., 1974; Hwang et al., 1975; Mailer & Hoffman, 1976). In biological systems, an important example of such complex formation will probably be hydrogen bonding. Griffith et al. (1974) have shown that lipid spin probes which are in contact with water will form hydrogen bonds between the water molecules and the NO· group, with the hydrogen bond producing an increase in the hyperfine coupling constant. This interaction was then used to demonstrate the existence of water penetration into lipid bilayers and to determine the shape of the hydrophobic barrier within the bilayer region of biological membranes (Griffith et al., 1974).

Humphries & McConnell (1976) have also shown that a nitroxide bound to specific rabbit antibodies exhibits an unusually large hyperfine separation and have suggested that hydrogen bonding may play a role in the immobilization of the nitroxide within the antibody binding site. Lozos & Hoffman (1974) and Mailer & Hoffman (1976) have also found the limiting hyperfine splitting of di-*tert*-butyl nitroxide hydrogen bonded to surface hydroxyls of silica to be about 10 G larger than usually observed. More recently we have reported that the spin-label hyperfine separation of Mal-6[1] labeled HbCO exhibits a strong temperature dependence which is suggestive of hydrogen bonding (Johnson, 1979a). Direct evidence for nitroxide hydrogen bonding has also been demonstrated by Hwang et al. (1975), who have shown that

† From the Department of Medicinal Chemistry, University of Illinois at the Medical Center, Chicago, Illinois 60680, and the Division of Biological and Medical Research, Argonne National Laboratory, Argonne, Illinois 60439. *Received May 9, 1980.* Supported in part by grants from the Research Corporation and the National Institutes of Health (HL-23697) and by the U.S. Department of Energy under Contract No. W-31-109-ENG-38 (at ANL). This work was done in part during the tenure of an Established Investigatorship from the American Heart Association and with funds contributed in part by the Chicago affiliate.

[1] Abbreviations used: Hb, hemoglobin; HbCO, carbonmonoxy liganded ferrous Hb; metHb, ferric Hb; Mal-6, 4-maleimido-2,2,6,6-tetramethylpiperidinyloxy; Mal-5, 3-maleimido-2,2,5,5-tetramethyl-1-pyrrolidinyloxy; 5-doxylstearate, 2-(3-carboxypropyl)-4,4-dimethyl-2-tridecyl-3-oxazolidinyloxy; Tempone, 2,2,6,6-tetramethyl-4-piperidone *N*-oxide; DPPC, dipalmitoylphosphatidylcholine; EPR, electron paramagnetic resonance; ST-EPR, saturation transfer EPR; ELDOR, electron double resonance.

0006-2960/81/0420-3319$01.25/0

perdeuterated Tempone in an ethanol glass at low temperature exhibits a two-component spectrum, with the two components exhibiting different hyperfine separations. The component with the larger hyperfine separation was attributed to a Tempone–ethanol hydrogen-bonded complex, while the smaller hyperfine separation component was attributed to Tempone in the absence of hydrogen bonding.

Since hydrogen bonding produces significant spectral effects, it would appear to be an important aspect of the interaction of spin-labels with a wide diversity of biological systems. A major barrier to a direct study of this hydrogen-bonding interaction has been the problem of separating the spectral effects of nitroxide motion from those due to the bonding interactions. In the present communication, we demonstrate that this problem may be partially circumvented through detailed spectral studies under conditions where the spin-label motional freedom is strongly restricted. Using various spin-labeled hemoglobin derivatives and a lipid system with an incorporated spin probe, we find that substantial thermodynamic information about the hydrogen-bonding interaction may be obtained from the temperature dependence of the rigid limit hyperfine separation. The thermodynamics of this interaction under various experimental conditions suggest that hydrogen bonding may be a factor in the strong immobilization of spin-labels by macromolecules. The temperature dependence of the hydrogen-bonding interaction is also seen to have implications for other biophysical spin-label measurements.

Materials and Methods

Sample Preparation. Blood samples were obtained from the University of Illinois Hospital Blood Bank; hemoglobin was prepared from the pooled blood samples by the mehods of Abraham et al. (1975) and kept under CO atmosphere until use. Mal-5 and Mal-6 (Syva Corp.) spin-labeling of Hb followed previously published procedures (Johnson, 1978). Hb was desalted by running through a column of Rexyn-I-300 (Fisher). After being desalted, Hb solutions were concentrated by ultrafiltration (Amicon). Hb concentrations were determined from the visible absorption bands at 540 and 569 nm (Antonini & Brunori, 1971).

For Hb studies, spin-labeled Hb and unlabeled Hb at concentrations of 20–30% were mixed in a molar ratio of 1:2 and then immobilized either by simply freezing the solutions or by precipitating the Hb out of solution with saturated (at 4 °C) ammonium sulfate at pH 7. The freezing process was carried out either by placing the sample into the EPR variable temperature Dewar and slowly lowering the temperature through the freezing point or by plunging the sample into liquid nitrogen and then inserting it into the EPR variable temperature Dewar and allowing it to warm up to the appropriate temperature; the method used is noted where appropriate. The lyophilized Hb sample was also prepared from Mal-6-labeled Hb diluted with unlabeled Hb in a molar ratio of 1:2. After lyophilization, the dry powder was packed in a quartz EPR tube and evacuated at room temperature for 24 h to remove any residual bound water. The tube was then sealed under vacuum.

Lipid samples were prepared by dissolving DPPC in reagent grade chloroform, adding 5-doxylstearate (Syva Corp.) spin probe in a lipid to probe weight ratio of 400:1, mixing thoroughly, and evaporating most of the chloroform under nitrogen. The remainder of the chloroform was removed by placing the sample under high vacuum overnight. An aliquot of this powder sample was then packed into a capillary tube, evacuated again for 24 h, and sealed under vacuum. Aqueous multilayer dispersions were prepared by adding excess 0.01 M sodium phosphate buffer, pH 6.6, and alternately warming the sample to about 60 °C, incubating for 2–3 min, and vortexing vigorously for about 2 min. This cycle of heating and vortexing was repeated about 10 times.

Spectroscopic Measurements. Spin-label EPR spectra were measured on a Varian E-112 spectrometer equipped with an E-257 variable temperature accessory. Samples were contained in 50- or 100-μL sealed capillary pipets and were centered in the Dewar by specially constructed holders.

For normal absorption (first harmonic, in-phase) spectra, microwave power settings of 1 mW at temperatures above −75 °C and 0.2 mW at temperatures below −75 °C were used unless noted otherwise. Care was taken to ensure that the power setting was always low enough to eliminate any saturation-induced line shape distortion. No line broadening was observed at a modulation level of 1 G; thus this modulation amplitude was used at all temperatures. The hyperfine separations were measured by expanding the spectrum to approximately 10 times vertical full scale on the chart recorder and then locating the positions of the hyperfine extremal peaks. At this expansion, the peak positions are quite well-defined. For minimization of any field drift effects, the field was scanned in both the increasing and decreasing directions, and the two values were averaged. A 100-G sweep width was used for all measurements. The sweep width was calibrated from the residual Mn^{2+} in SrO (Bolton et al., 1972). The relative precision of one measurement with respect to another is estimated to be within ±0.3 G.

Second harmonic saturation transfer spectra were measured by using the self-null procedure of Thomas et al. (1976). The modulation amplitude and frequency settings were 5 G and 50 kHz, respectively, with phase-sensitive detection occurring at 100 kHz. The microwave power used depended on the specific sample conditions. For the dry powder DPPC sample, the quartz variable temperature Dewar appeared to intensify the microwave field by about a factor of 2, and it was assumed that the sample produced negligible effects on the cavity Q. Thus a power setting of 0.2 mW was used for locating the phase null, and a power setting of 30 mW was used for observing the out-of-phase signal. The 30-mW setting was estimated to give approximate correspondence to the 63-mW standard setting used by Thomas et al. (1976). The frozen samples appeared to lower the cavity Q slightly; thus a power setting of 40 mW was used for observing the out-of-phase signals. For the aqueous DPPC samples above the freezing point, the effective power was determined by comparing the spectra of Mal-6-labeled HbCO in glycerol–water solutions at various power levels with the calibration spectra of Thomas et al. (1976). With the sample geometry used here, a setting of approximately 50 mW appeared to correspond to an effective power of 63 mW. In the present study, the interest is primarily in determining the effect of temperature upon the individual samples rather than in comparing different types of samples. Thus more exacting efforts to standardize the effective power level were not considered necessary.

The temperature was measured by using a copper–constantan thermocouple and a Honeywell Model 2746 potentiometer. The relative precision of individual temperature measurements at temperatures above about −80 °C was approximately ±0.5 °C, with an estimated overall accuracy of ±1 °C. At the lowest temperatures, the uncertainties are estimated to be about a factor of 2 larger.

Hydrogen-Bond Model. Hydrogen-bond formation by the NO· group is assumed to produce a dual-valued A_{zz} parameter, one value associated with the bonded state and one associated

with the dissociated state. An equilibrium between the two states which is temperature dependent and rapid on the EPR time scale will then also produce a temperature-dependent hyperfine separation.

The environment of a tightly bound spin-label which is located within a fixed binding site will be very similar to a solid-state or crystalline environment. Thus for a hydrogen-bond equilibrium

$$\text{NO}\cdot\text{–HX} \rightleftharpoons \text{NO}\cdot + \text{HX}$$

we define the dissociation constant

$$K = [\text{NO}\cdot]/[\text{NO}\cdot\text{–HX}] \quad (1)$$

where NO· and NO·–HX are respectively the unbonded and hydrogen-bonded nitroxide fractions.[2] As usual, the Gibbs free energy is related to K by

$$\Delta G = -RT \ln K = \Delta H - T\Delta S \quad (2)$$

where ΔG is the change in free energy, R is the universal gas constant, T is the absolute temperature, ΔH is the change in enthalpy, and ΔS is the change in entropy.

In developing an expression for the temperature dependence of the observed hyperfine separation, $2A_{zz}(T)$, we assume that the separation between the unbonded and hydrogen-bonded states differs by some increment, Δ, or

$$2A_{zz}(\text{NO}\cdot) = 2A_{zz}(\text{NO}\cdot\text{–HX}) - 2\Delta_{zz} = 2A_{zz}^0 - 2\Delta_{zz}$$

We also assume that the two states are in rapid equilibrium so that line averaging occurs. Under those conditions, the separation at any temperature will simply be the weighted average of the separations for the two states, or

$$2A_{zz}(T) = 2A_{zz}^0\frac{[\text{NO}\cdot\text{–HX}]}{[\text{NO}\cdot] + [\text{NO}\cdot\text{–HX}]} + (2A_{zz}^0 - 2\Delta_{zz})\frac{[\text{NO}\cdot]}{[\text{NO}\cdot] + [\text{NO}\cdot\text{–HX}]}$$

This reduces to

$$2A_{zz}(T) = 2A_{zz}^0 - 2\Delta_{zz}\frac{1}{1 + K^{-1}}$$

and

$$2A_{zz}(T) = 2A_{zz}^0 - 2\Delta_{zz}\left[1 + \exp\left(\frac{\Delta H}{RT} - \frac{\Delta S}{R}\right)\right]^{-1} \quad (3)$$

[2] The mass action expression is commonly written in the form

$$K_D = [\text{NO}\cdot][\text{HX}]/[\text{NO}\cdot\text{–HX}]$$

provided that all constituents of the reaction are acting as essentially ideal solutes. However, if HX and NO· are effectively different moieties of a larger molecular complex, then dilution of the solution does not reduce their probability of interaction since the molecular complex will "hold" them in a constant geometry, independent of concentration. Under these conditions, the proper expression for K_D is given by eq 1. Alternatively, if the initial proton donor concentration is very much larger than the initial nitroxide concentration, i.e., $[\text{HX}]_0 >>> [\text{NO}\cdot]_0$, as would be the case if HX were the bulk water, then $[\text{HX}] \simeq [\text{HX}]_0$, and

$$[\text{NO}\cdot]/[\text{NO}\cdot\text{–HX}] = K_D/[\text{HX}] \simeq K_D/[\text{HX}]_0 = K_D'$$

The result of this approximation is that the apparent entropy change of K_D' will be shifted from that of K_D. For the frozen solutions of desalted Hb, the only proton donors available would appear to be water molecules or some element of the protein matrix since they are the only constituents of the solution. Furthermore, if we calculate the equivalent expressions 2 and 3 from the general mass action expression, we find that, in addition to being temperature dependent, $2A_{zz}(T)$ would also be strongly dependent on $[\text{NO}]_0$. Such a dependence is not consistent with the experimental data of Figures 2 and 3, as discussed in the text. Thus the definition (eq 1) given above appears to be appropriate.

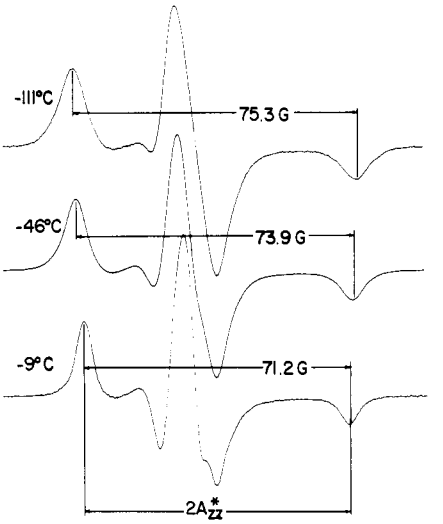

FIGURE 1: Spectra of Mal-6-labeled HbCO frozen in solution. The temperature and hyperfine separation for each spectrum are as shown. The line broadening observed as the temperature decreases may be due to a temperature dependence in the inhomogeneous broadening (Johnson, 1978, 1979b).

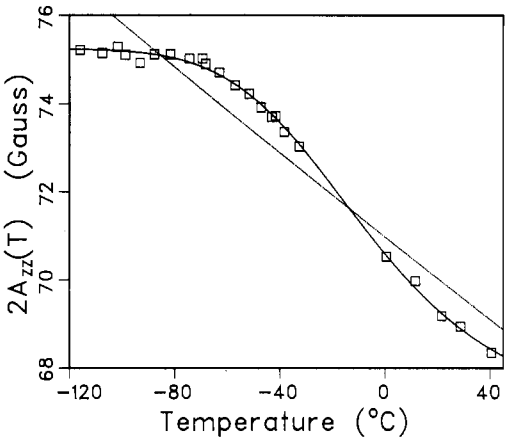

FIGURE 2: Observed hyperfine separation of Mal-6-labeled HbCO which has been immobilized by ammonium sulfate precipitation out of solution. The data shown are the combined results from two different experiments. The dotted line represents the best fit of the torsional oscillation model (eq 4 and 5) to these data. The solid line represents the best fit of the hydrogen-bond model (eq 3).

The parameters for this model and for the torsional oscillation model described in the Appendix were derived from the experimental data by nonlinear least-square methods by using the nonlinear routines of the SAS package (Barr et al., 1976).

Results

Experimental Data

The spectra in Figure 1 indicate that the hyperfine separations in frozen solutions of Mal-6-labeled Hb increase significantly as the temperature is decreased from −9 to −111 °C. This temperature behavior is shown in more detail in Figure 2, from which it can be seen that the hyperfine separation of Mal-6-labeled HbCO which has been immobilized by ammonium sulfate precipitation changes by approximately 7 G over the temperature range −120 to +40 °C. This temperature behavior is also rather nonlinear. At temperatures below about −70 °C, the hyperfine separation exhibits a nearly constant value of approximately 75 G. Above −70 °C, it exhibits a rapid decrease as temperature increases; this behavior continues up to at least +40 °C. Previous ST-EPR studies of this system have also shown that there is virtually no change in the ST-

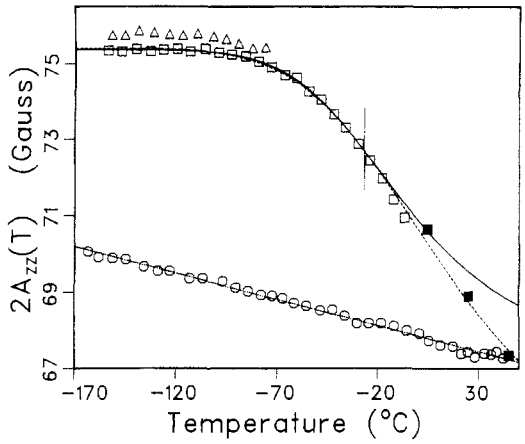

FIGURE 3: Comparison of the hyperfine separation temperature dependencies for Mal-6-labeled Hb which has been immobilized by the following methods. The points (□) are for HbCO which has been frozen in solution at low ionic strength; the points (■) are from previous work (Johnson, 1979a) in which the rigid limit hyperfine separation was obtained by extrapolating the hyperfine separations observed for Mal-6-labeled HbCO dissolved in sucrose solutions of differing viscosities to that which would be observed in the limit of infinite viscosity. The slight discontinuity which appears to occur at about 0 °C between the viscosity extrapolated data and the frozen sample data may be due either to the somewhat high power (5-mW setting) used in the viscosity extrapolation procedure or to a partial elimination of librational motion effects in the viscosity extrapolation procedure. The dashed line is the best fit of the hydrogen-bond model (eq 3) to the aqueous Mal-6 HbCO data over the full temperature range, −160 to +45 °C. Since librational motion is likely to be affecting the high temperature data, a regression was also performed by using a high temperature cutoff of −25 °C; the results are shown as the solid line (the vertical line at ~−25 °C notes this cutoff). The points (○) are from Mal-6-labeled HbO_2 which has been lyophilized and sealed under vacuum. The dotted line is a best fit of the torsional oscillation model (eq 1 and 2) to that data. It is interesting to note that the value of $2A_{zz}^0$ predicted for the lyophilized Hb is almost exactly half way between the values of $2A_{zz}^0$ and $2A_{zz}^0 - 2\Delta_{zz}$ predicted by the hydrogen-bond model from the low temperature aqueous HbCO data.

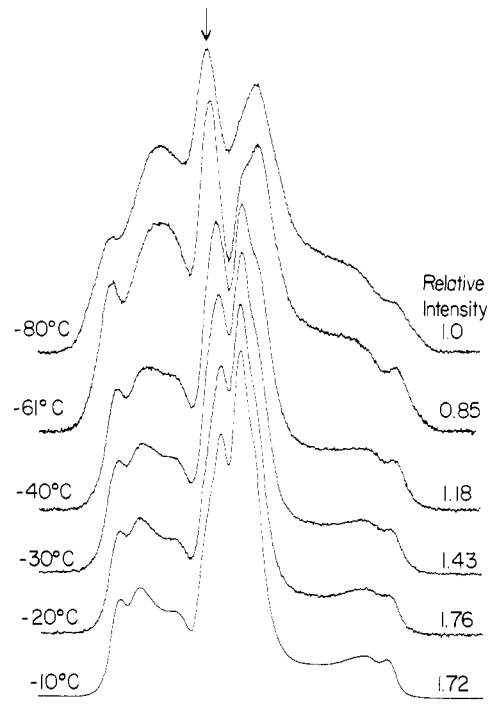

FIGURE 4: ST-EPR spectra of Mal-6-labeled HbCO frozen in solution at low ionic strength. Temperatures are as shown. The values shown for relative intensity are the relative intensities, between spectra, of the peak marked by the arrow, with the −80 °C spectrum serving as reference with a relative intensity of 1.0.

EPR spectral shape between 1 and 40 °C and that any large amplitude motion by the label is slower than can be reliably measured by second harmonic ST-EPR methods (Johnson, 1978).

The data for Mal-6-labeled HbCO which has been immobilized by slow freezing are shown as the open squares in Figure 3. The data shown as the solid squares above 0 °C in Figure 3 are taken from previous work (Johnson, 1979a) in which the rigid limit hyperfine separation was obtained by measuring the hyperfine separation of Mal-6-labeled HbCO in solutions of different viscosities and extrapolating to infinite viscosity to obtain the rigid limit hyperfine separation (i.e., the hyperfine separation which would be observed in the absence of HbCO rotational diffusion). The behavior of the data for the low ionic strength HbCO system (slow freezing) is quite similar to that of the precipitated HbCO in Figure 2, with the exception that the high-temperature (+45 °C) hyperfine separation is about 1 G less for the low ionic strength sample than for the ammonium sulfate precipitated sample (+40 °C). This also indicates that the temperature dependence of the hyperfine separation is not sensitive to the concentration of the spin-labeled Hb. In the viscosity extrapolation data, the Hb concentration is about 3% (w/v); in the frozen sample, it is about 15%. The ammonium sulfate precipitated Hb is a two-phase system with the condensed Hb volume fraction probably at about 50–70% (Alpert & Banks, 1976; Jones et al., 1978).

After the HbCO sample was frozen, it was noted that the detector current, and thus the sample dielectric constant, continued to change substantially as the temperature was decreased until about −25 °C, where it reached a steady value. This was taken to indicate that the hydration shell around the protein does not fully freeze until about −25 °C. (For distilled water, the detector current changes abruptly upon freezing, but does not change further as temperature decreases.)

It was also noted that the observed hyperfine separation depended slightly on the method of freezing. Data for an HbCO sample which was "flash" frozen by plunging the capillary into liquid nitrogen and then placed in the variable temperature Dewar (the triangles in Figure 3) exhibit hyperfine separations about 0.4 G larger than those of the slow-frozen sample at low temperature. No attempt was made to determine the source of this effect.

Exchanging D_2O for H_2O (data not shown) appeared to reduce the asymptotic low-temperature limit for the hyperfine separation by about 0.3 G. At temperatures above about −90 °C, the two data sets appeared to converge; from about −40 up to 0 °C they were indistinguishable. Thus the only significant effect of substituting D_2O for H_2O appears to be a slight reduction in the low temperature limiting hyperfine separation.

ST-EPR spectra for the frozen Mal-6-labeled HbCO system are shown in Figure 4. There appears to be substantial line broadening and some changes in relative spectral intensities as the temperature is lowered from −10 to −80 °C. However, even at −10 °C, the spectral parameters defined by Thomas et al. (1976) all indicate any motions to have apparent correlation times of 10^{-3} s or longer.

Figure 5 demonstrates that a strong temperature dependence of the hyperfine separation is not unique to Mal-6-labeled HbCO. Frozen solutions of Mal-6-labeled deoxy-Hb, cyanomet-Hb, and aquomet-Hb also exhibit behavior quite similar to that of the frozen Mal-6-labeled HbCO. HbCO labeled with the five-membered nitroxide ring analogue of Mal-6, i.e., Mal-5, likewise exhibits similar behavior with the exception that the asymptotic low temperature hyperfine separation is

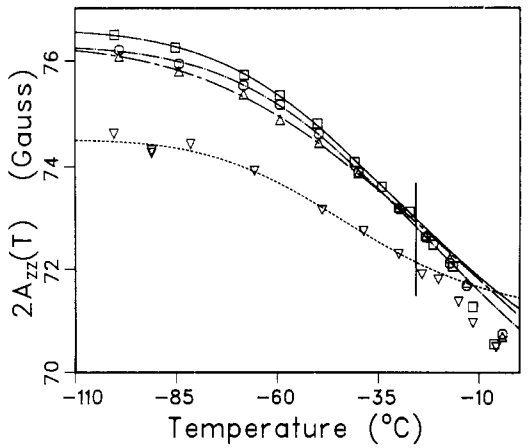

FIGURE 5: Observed hyperfine separations for Mal-6- and Mal-5-labeled Hb derivatives in frozen solution. The smooth lines are the best fits of the hydrogen-bond model (eq 3) to the experimental data, again using a high temperature cutoff of −25 °C (vertical line). The various systems are Mal-5-labeled HbCO (---) (▽), Mal-6-labeled cyanomet-Hb (−·−) (△), Mal-6-labeled aquomet-Hb (−·−) (○) and Mal-6-labeled deoxy-Hb (—) (□).

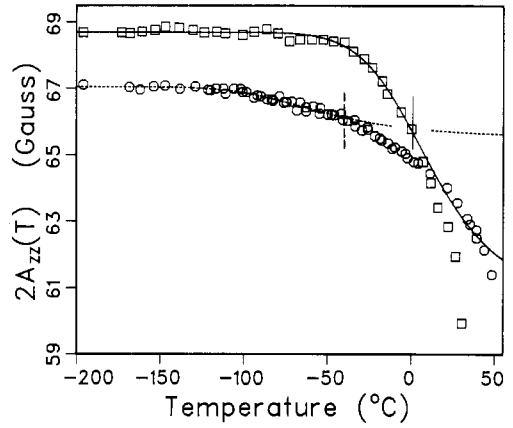

FIGURE 6: Observed temperature behavior of the hyperfine separation for 5-doxylstearate incorporated into aqueous DPPC dispersions (□) and diluted into DPPC as a dry powder (○). The smooth lines are the best fits of the hydrogen-bond model to the data using the high temperature cutoffs shown by the vertical lines.

about 2 G smaller than is observed for the six-membered ring systems.

In contrast, the hyperfine separation for lyophilized Hb (shown as the circles in Figure 3) changes by less than 3 G over the temperature range −170 to +45 °C. Furthermore, the change in hyperfine separation for lyophilized Hb appears to be almost perfectly linear with temperature.

The temperature behavior of the hyperfine separation for 5-doxylstearate incorporated into a bilayer dispersion of DPPC is shown as the squares in Figure 6. The behavior is quite similar to that observed for the aqueous Hb systems, with the separation exhibiting an asymptotic low temperature limit slightly less than 69 G and decreasing rapidly with increasing temperature for temperatures above about −50 °C.

ST-EPR spectra for the 5-doxylstearate/DPPC aqueous dispersions are shown in Figure 7A for the temperature range −41 to +20 °C. The spectra indicate the existence of a significant increase in nitroxide motion for temperatures above 0 °C. Comparison with the calibration spectra of Thomas et al. (1976) yields three motional correlation times corresponding to parameterizations of the low-, central-, and high-field regions of the spectrum. At 20 °C, the central region of the spectrum corresponds to a correlation time $\tau \sim 10^{-5}$ s. The low- and high-field regions of the spectrum indicate motional rates about an order of magnitude slower than this.

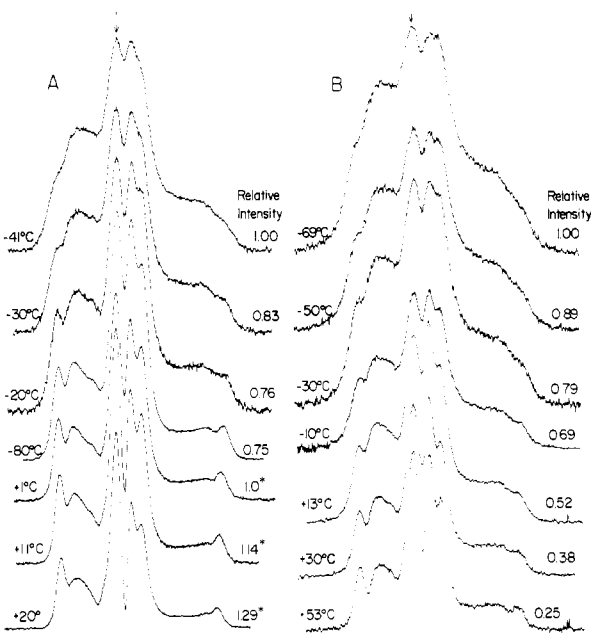

FIGURE 7: (A) ST-EPR spectra of the aqueous DPPC/5-doxylstearate system at the temperatures shown. Relative spectral intensities of the peak marked by the arrow are shown at the right side of the spectra. The relative intensities of the −8, −20, and −30 °C spectra are referenced to the −41 °C spectrum. The relative intensities of the +20 and +12 °C spectra are referenced to the +1 °C spectrum (starred values). Relative intensities above and below the freezing point were not determined. (B) ST-EPR spectra of 5-doxylstearate diluted into a dry powder of DPPC. Relative intensities are referenced to the −69 °C spectrum. Note that the marked loss in intensity as temperature increases differs strongly from the behavior of the two aqueous systems (part A and Figure 4).

The dry powder system, in which 5-doxylstearate has been diluted in DPPC, exhibits the temperature behavior shown as the circles in Figure 6. The behavior is qualitatively similar to that observed for the aqueous DPPC dispersion and Hb systems, with an asymptotic low-temperature limit of about 67 G and a decreasing separation for temperatures above about −120 °C. The detailed behavior of the temperature-induced decrease, however, appears somewhat different than for any of the other systems. Between −120 and −40 °C, the decrease in hyperfine separation appears to be relatively gradual and approximately linear with temperature. Above −40 °C, the rate of decrease accelerates rapidly with increasing temperature.

ST-EPR spectra for this system are shown in Figure 7B for the temperature range −69 to +53 °C. From this figure, it can be seen that the spectral "turning points" become much more sharply defined and spectral intensity between "turning points" is reduced somewhat (particularly in the center) as the temperature is increased. [See Thomas et al. (1976), particularly Figure 3, for a discussion of ST-EPR spectral features.] The spectral intensity is also reduced by slightly more than a factor of 4 between −69 and +53 °C.

Data Analysis

Hydrogen Bonding. If we assume that the label is essentially motionless, but that it may be hydrogen bonded to a proton donor within its binding site, we would expect to observe two values for the hyperfine separation, one corresponding to the dissociated state and one corresponding to the bonded state. Coordination of this nature would shift charge density more toward the oxygen and spin density more toward the nitrogen of the NO· group than would be observed for the nonbonded state. Thus the hydrogen-bonded state would exhibit the larger hyperfine separation. The bonded state would also be expected

Table I: Best-Fit Model Parameters for Various Experimental Systems

(A) Hydrogen Bond Model[a]

exptl system	$2A_{zz}^{0}$ (G)	$2\Delta_{zz}$ (G)	ΔH (kcal/mol)	ΔS (cal/mol·K)
precipitated Mal-6 HbCO	75.24 ± 0.04	8.54 ± 0.41	5.06 ± 0.26	18.9 ± 1.2
desalted Mal-6[b] HbCO ($T \leq 45$ °C)	75.41 ± 0.04	12.38 ± 0.93	4.01 ± 0.21	13.7 ± 1.0
desalted Mal-6[c] HbCO ($T \leq -25$ °C)	75.38 ± 0.02	8.20 ± 2.81	4.60 ± 0.37	17.2 ± 2.4
aqueous DPPC/5-doxylstearate ($T \leq 0$ °C)	68.69 ± 0.02	8.08 ± 4.12	7.37 ± 1.07	25.9 ± 5.4
powder DPPC/5-doxylstearate ($T \leq 40$ °C)	67.04 ± 0.03	1.56 ± 0.61	3.24 ± 0.79	14.6 ± 5.0

(B) Torsional Oscillation Model[d]

system	A_{zz}^{0} (G)	E_A (kcal/mol)
lyophilized Mal-6 HbCO	35.82 ± 0.02	2.53 ± 0.04

[a] Equation 3. [b] This regression includes all of the aqueous HbCO data in Figure 3 and thus probably reflects some librational motion influence at high temperature in addition to hydrogen-bonding effects. [c] A high-temperature cutoff of −25 °C was used in order to minimize any librational motion effects. Moving the cutoff somewhat lower in temperature did not significantly alter the results. A comparison of the ΔH, ΔS, and Δ_{zz} parameters derived by using this cutoff with those derived by using the 45 °C cutoff also indicates that changing the cutoff produces slight changes in ΔH, moderate changes in ΔS, and rather large changes in $2\Delta_{zz}$. Thus values of the enthalpy of bond formation, ΔH, are probably fairly reliable, and values of the entropy change, ΔS, are probably moderately reliable, but values of $2\Delta_{zz}$ should be treated with some caution. [d] Equations 4 and 5 in the text.

to be lower in energy than the dissociated (nonbonded) state. The absence of any observed splitting in the experimentally observed hyperfine extremal lines over the entire temperature range indicates that the transition rate between the two states must be rapid compared to the resonance separation between the two states. The observed value would thus be an average value for the two states. Under these circumstances the temperature dependence of the hyperfine separation should be given by eq 3. The best fit of this expression for the ammonium sulfate precipitated Mal-6-labeled Hb is shown as the solid line in Figure 2; values for the best fit parameters are given in Table I. From a comparison of this best fit line with the experimental data, it appears that the hydrogen-bond model is adequate to explain all of the observed hyperfine separation temperature dependence for the precipitated Mal-6-labeled HbCO system. The previous ST-EPR study of this system (Johnson, 1978) provides further confirmation that nitroxide motion within its binding sites does not contribute significantly to the observed temperature dependence of the precipitated HbCO system.

The best fit of eq 3 to the low ionic strength aqueous HbCO data of Figure 3 is shown as the dashed line in that figure; values of the regression parameters are given in Table I. The fit appears to be quite good over the full temperature range from −160 to +45 °C. For this system, however, there is a much higher likelihood of nitroxide librational motion contributing to the observed temperature dependence, particularly at high temperature. Previous work has shown that librational motion contributes significantly to the hyperfine extremal line widths at temperatures above 0 °C (Johnson, 1978). Using ELDOR methods, Hyde et al. (1975) have also shown the existence of significant librational motion effects for Mal-6 labeled HbO_2 frozen in ice at about −10 °C. The most obvious approach for avoiding such librational contributions is simply to exclude the high temperature data in performing the regression of eq 3. Since the freezing process appears to be complete at about −25 °C, this was used as a high temperature cutoff. The results of this regression are given in Table I and are shown as the solid line in Figure 3. Moving the cutoff to an even lower temperature did not alter the results significantly. From Figure 3 it can be seen that this second regression fits the low temperature data quite well. At high temperature, however, the regression curve predicts higher values for the hyperfine separation than are experimentally observed, with the discrepancies increasing as temperature increases. Behavior of this nature would be expected if the amplitude of nitroxide librational motion increased as the ice structure around the protein begins to melt and permit some flexibility in protein conformation. It is also of interest to note that all of the regression parameters for the low temperature regression of the frozen HbCO are quite close to those predicted for the ammonium sulfate precipitated HbCO system. This is further confirmation that the temperature dependence below −25 °C arises from essentially only hydrogen bonding but that librational motion also begins to affect the hyperfine separation at higher temperatures in the low ionic strength system.

By use of the −25 °C high temperature cutoff, regressions of the hydrogen bond model, eq 3, were also performed for the Mal-5-labeled HbCO and Mal-6-labeled deoxy-Hb, cyanomet-Hb, and aquomet-Hb data in Figure 4. The results are shown as the various lines in that figure. The principal points of interest for these systems are that the different Mal-6-labeled Hb derivatives exhibit thermal dependencies which are quite similar to each other, but which differ in detail, and that the Mal-5-labeled HbCO exhibits a temperature dependence which is qualitatively quite similar to those of the Mal-6-labeled derivatives.

The thermal behavior of the hyperfine separation for the aqueous dispersion of DPPC with incorporated 5-doxylstearate (Figure 6) is quite similar to that of the aqueous Hb systems. In this system, we again face the problem of separating motional effects from those due to possible hydrogen bonding. From the ST-EPR spectra of Figure 7A, it appears that there is a rather substantial increase in nitroxide motion as the temperature increases above 1 °C. At this temperature and below, however, the spectral parameters of Thomas et al. (1976) all indicate correlation times of 10^{-4} s or longer. This is 1–2 orders of magnitude longer than the maximum correlation time at which motionally induced changes in the hyperfine separation should be observable (McCalley et al., 1972; Goldman et al., 1972). Thus 0 °C was somewhat arbitrarily chosen as a high-temperature cutoff for the regression analysis of eq 3. The results are shown as the solid line in Figure 6; the regression parameters are given in numerical form in Table I. From this figure it can be seen that the fit to the data below 0 °C is well within experimental uncertainty. As the temperature increases above 0 °C, there is an increasing discrepancy between the hydrogen-bond regression curve and the experimentally observed hyperfine separations. Such a discrepancy would be expected, however, due to the increasing motional contribution which can be deduced from the ST-EPR spectra of Figure 7A. Thus the behavior of this system is consistent with the thermal behavior of the hyperfine separation being dominated by hydrogen bonding at low temperature and with motional effects contributing increasingly at high temperature.

As was previously noted, the thermal behavior of the hyperfine separation for the dry powder DPPC system, also shown in Figure 4, is qualitatively similar to that of the aqueous DPPC and Hb systems. In fitting the hydrogen-bond model to the data, however, it was found that the regressions did not converge for high-temperature cutoffs above −30 °C. The ST-EPR spectra of Figure 7 would initially suggest that the motion is quite slow even up to +53 °C. However, there is also a substantial decrease in spectral intensity as the temperature increases, with the intensity at +53 °C reduced to approximately 25% of that at −69 °C. This reduction in spectral intensity is quite suggestive of the existence of high-frequency, limited amplitude nitroxide motion. The powder DPPC system is almost certainly highly disordered. Thus it is likely that the nitroxide probe will exist in a variety of environments, some of which may be structurally quite restricted and others of which may be structurally rather flexible. In an attempt to minimize any motional contributions to the spectral behavior, high temperature cutoffs of −50 and −40 °C were tested for the regression and found to yield convergence with essentially equivalent results. The best fit from this regression is shown as the dashed line in Figure 5; numerical values for the regression parameters are given in Table I. From this figure, it can be seen that the calculated curve fits the experimental data quite well up to the −40 °C cutoff. However the predicted value of approximately 1.6 G for $2\Delta_{zz}$, the difference in hyperfine separation between the hydrogen-bonded and nonbonded states, is much smaller than observed for any of the aqueous systems. Interpretation of this value is also further complicated by the probable heterogeneity of nitroxide environments within the powder DPPC system.

Librational Motion Effects. The thermal behavior of the hyperfine separation for the lyophilized sample of Mal-6-labeled Hb (Figure 3) differs substantially from that of any of the aqueous Hb systems. The hydrogen-bond model does not provide a good fit for this system. The linearity of these data, compared to that of the aqueous systems, suggests that a different mechanism is probably giving rise to this temperature behavior. Librational motion of the nitroxide within its binding site would be one plausible mechanism. The spectra of Mal-6-labeled HbCO in solution have shown that full rotation of the nitroxide ring is inhibited within the Hb binding site (McCalley et al., 1972). However, the possibility of small amplitude motional fluctuations or oscillations of the nitroxide ring within its binding site is thermodynamically quite plausible and has been previously considered (Hyde & Thomas, 1973; Hyde et al., 1975; Johnson, 1978). Small amplitude fluctuations of the N—O· bond orientation with respect to the C—N—C plane of the nitroxide ring would also produce effects equivalent to torsional motion of the full ring. In the Appendix, it is shown that the effect of such motion would be to produce a temperature-dependent hyperfine separation of the form

$$2A_{zz}(T) = A_{zz}^{0}(1 + \cos \Theta) \quad (4)$$

where

$$\Theta = (RT/E_A)^{1/2} \quad (5)$$

Θ is the half-angle of oscillation, E_A is a parameter characterizing the torsional energy barrier, and $2A_{zz}^{0}$ is the hyperfine separation in the absence of motion.

The best fit of this model to the lyophilized Hb data is shown as the dotted line in Figure 3, from which it can be seen that the fit is excellent. Values of the regression parameters are given in Table I. For comparison, the best fit of this model to the ammonium sulfate precipitated Hb data is shown as the dotted line in Figure 2. The fit is again nearly linear and clearly does not correspond to the experimental data for any of the aqueous systems.

Discussion

The results described above provide evidence for the existence of nitroxide hydrogen bonding within biomolecular systems. In particular, the high ionic strength system of Mal-6-labeled HbCO precipitated by saturated ammonium sulfate exhibits a substantial temperature-dependent hyperfine separation for which the hydrogen-bond model provides a very good fit at all temperatures. In contrast, a librational motion model provides a very poor fit to the data. Furthermore, ST-EPR studies of the precipitated HbCO system indicate that the high ionic strength suppresses residual nitroxide motion to the point where it is not readily detectable even at temperatures up to +40 °C (Johnson, 1978). Thus the observed temperature dependence must be explained either as an intrinsic property of the nitroxide itself or as a secondary effect resulting from an interaction of the nitroxide with some group in its environment. The almost perfectly linear temperature dependence of the hyperfine separation observed for lyophilized Mal-6-labeled HbCO, however, indicates that the semisigmoidal behavior observed in the aqueous Hb systems cannot be an intrinsic property of the nitroxide. Likewise, the slightly differing temperature dependencies observed for Mal-6-labeled deoxy-Hb and the two metHb derivatives indicate that the nitroxide is quite sensitive to nearby environmental structure and suggest that the temperature dependence is the result of a specific interaction between the nitroxide and some group within its environment. The most plausible interaction which can satisfy these requirements is hydrogen-bond formation between the nitroxide NO· group and a proton donor within its immediate environment. Nitroxides have also been shown to form hydrogen bonds in a number of other systems, and the enthalpies of bond formation of 4.6–5.1 kcal/mol for the aqueous Hb systems and about 7.4 kcal/mol for the aqueous DPPC system are consistent with the range of about 4.5–7.9 kcal/mol observed for the H bonding of various proton donors to model nitroxides (Lim & Drago, 1971; Morishima et al., 1973). Thus a temperature-dependent hydrogen-bonding equilibrium would appear to be a very plausible explanation for the low temperature spectral behavior observed in these studies.

The present work also provides some indirect evidence as to the identity of the nitroxide coordination partner in the aqueous Hb systems. The principal possibilities include a water molecule which might be located within the label binding site, an amide group on the peptide backbone, or a group on one of the polar side chains. The observation that both the Mal-6 and Mal-5 labels exhibit similar bonding to HbCO argues for structural flexibility of the coordination partner since the ring geometries differ significantly between the two labels. The sensitivity of the hydrogen-bond characteristics to protein structure (Figure 5), however, suggests the existence of a direct link between the NO· group and some element of the protein matrix. Bonding to a side chain thus appears to be most likely; a water molecule which is hydrogen bonded to both the NO· group and to some group within the label binding site might also meet these requirements. Within the aqueous DPPC systems, Griffith et al. (1974) have previously given evidence indicating that the nitroxide coordination partner is a water molecule.

These results also suggest that torsional oscillation or librational motion plays a significant role in the high temperature hyperfine separation behavior for most of the systems

studied here. For example, the experimentally observed hyperfine separation for the Mal-6-labeled HbCO system shown in Figure 3 is about 1.5 G smaller than that predicted by the low temperature regression. From this difference between the observed separation and the separation predicted in the absence of librational motion, eq 4 can be used to calculate an approximate half-angle of librational motion as $\Theta \simeq 17°$. Nitroxide motional averaging over a solid angle of this magnitude will be equivalent to averaging over only about 4% of a half-sphere; thus the effect will be to decrease the apparent hyperfine separation slightly, but produce little change in the overall spectral shape.

The lyophilized HbCO probably permits the most accurate calculation of librational motion amplitude. At 42 °C, the highest temperature measured for this system, the half-angle of librational motion $\Theta \simeq 28°$. Nitroxide motional averaging over this solid angle will still provide averaging over only about 12% of a half-sphere. Thus the principal effect of this averaging will again be simply to decrease the apparent hyperfine separation somewhat, with little change in the overall spectral shape. From these brief calculations, it can be seen that the effects of librational motion may be rather substantial, but that direct detection of its existence will be rather difficult.

The model developed to describe torsional oscillation assumes that there is a constant, temperature-independent potential energy barrier to torsional motion. For the lyophilized HbCO system, this is probably a reasonably accurate assumption, and, in fact, the model is adequate to fully explain the observed temperature dependence for this system. However, in the frozen aqueous Hb systems, it appears likely that the ice structure around the protein will produce strong suppression of any nitroxide librational motion. As the temperature increases and the ice structure relaxes around the protein, the protein conformational flexibility will increase, probably also producing a rapid increase in the amplitude of librational motion. A similar situation will also exist in the aqueous DPPC dispersions. At low temperature, the lipid hydrocarbon chains will probably form a nearly rigid matrix for the nitroxide probe. As the temperature increases, there will be a gradual increase in the flexibility of the hydrocarbon region until the phase transition produces "melting" of the chains at 41 °C. Modifying the librational motion model to include such phase-transition effects is outside the scope of this work. Hence, no attempt has been made to develop a combined hydrogen bonding/librational motion model to describe the full range of temperature effects in the various systems.

The existence and strong temperature dependence of the hydrogen-bonding equilibrium observed in these studies have significant implications for several types of biophysical spin-label measurements. McConnel, Freed, and their co-workers have recently shown that the rate of spin-label rotational motion (for 10^{-8} s $\lesssim \tau_R \lesssim 10^{-6}$ s) may be determined from the decrease in hyperfine separation produced by rotational motion (McCalley et al., 1972; Goldman et al., 1972). For hemoglobin, however, the temperature-induced changes in $2A_{zz}$ over the temperature range ~0–~40 °C are nearly as large as those to be expected from rotational motion. Thus, as has recently been demonstrated, substantial temperature corrections are necessary before spin-label spectral parameters may be reliably used for calculating rates of rotational motion (Johnson, 1979b).

It has been previously suggested that hydrogen bonding is part of the binding mechanism by which nitroxides are bound to specific nitroxide antibodies (Humphries & McConnell, 1976). The present studies also provide tentative evidence that hydrogen bonding may contribute to the tight binding of Mal-5 and Mal-6 labels within the Hb protein matrix. Thus these results are suggestive that hydrogen bonding may, in general, be a contributing mechanism to the immobilization of spin-labels within macromolecular systems. The regression parameters given in Table I suggest, however, that it is probably not a dominant mechanism in spin-label immobilization. For example, the parameters for ammonium sulfate precipitated Hb yield $\Delta G = 0$ at about −5 °C. At room temperature, the hydrogen-bonding equilibrium will be moderately shifted toward the dissociation state.

Spin probe studies of lipid membrane systems may also be affected by temperature-dependent hydrogen bonding under some circumstances. The hydrogen-bonding equilibrium of 5-doxylstearate in the aqueous DPPC system exhibited the sharpest temperature dependence of any of the systems studied here. Thus it is probable, particularly in variable temperature studies, that changes in the hydrogen-bonding equilibrium will signficantly alter the various spectral parameters. Kang et al. (1979) have also recently questioned whether nitroxide spin probes incorporated into lipid bilayers may form hydrogen bonds with amide groups of membrane proteins, resulting in artifactual evidence for boundary lipid. Decisive evidence on this question is not yet available.

In summary, these studies provide evidence that hydrogen bonding is an important element in the interaction of nitroxide spin-labels and spin probes with biological systems. This interaction is quite sensitive to temperature and depends somewhat on the details of the experimental conditions. Work is in progress to develop systems which will permit a more detailed characterization of this interaction.

Acknowledgments

I thank Dr. Steven G. Danyluk for providing generous access to facilities in his laboratory at Argonne National Laboratory.

Appendix

Librational Motion Model. For a nitroxide ring which is tightly bound within a protein, it may still be possible for the ring to exhibit small amplitude oscillations about the minimum energy orientation within its binding site or for the NO· group to exhibit small amplitude oscillations with respect to the C–N–C plane of the nitroxide ring.

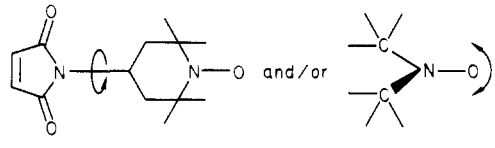

Small amplitude oscillations at high frequency (on the EPR time scale) of the nitroxide principal z axis will produce partial averaging of the A_{zz}, A_{yy}, and A_{xx} hyperfine tensor elements. A temperature dependence in the oscillation amplitude will, in turn, produce a temperature-dependent hyperfine separation.

In developing a description of this behavior, we consider the steric restrictions of the label binding site as being equivalent to an energy barrier, E_A, which hinders full 180° rotational motion of the nitroxide ring about the C–N bond between the nitroxide and maleimide moieties. Within the potential well formed by this energy barrier, however, we would expect thermal energy to prroduce torsional oscillations which are essentially harmonic in nature (provided that $kT \ll E_A$). As an approximation, we assume the potential well to be in the form

$$U = E_A(1 - \cos^2 \theta) \qquad \text{(A1)}$$

where θ is the spherical polar angle and E_A is the height of the rotational energy barrier imposed by the steric restrictions of the nitroxide binding site. The potential energy then has a value of $U = 0$ at $\theta = 0$, the minimum energy conformation, and a maximum value of $U = E_A$ at $\theta = 90°$. For small amplitude motion, the potential energy can be expanded in a power series about $\theta = 0$:

$$U = E_A[1 - (1 - \theta^2 + \tfrac{1}{3}\theta^4 \ldots)] = E_A(\theta^2 - \tfrac{1}{3}\theta^4 + \ldots)$$

To a first approximation, this gives

$$U \simeq E_A\theta^2$$

For two degrees of rotational freedom (no translational motion of the nitroxide ring), the equation of motion is then

$$kT = \tfrac{1}{2}I(d\theta/dt)^2 + E_A\theta^2$$

where k is Boltzmann's constant, T is the absolute temperature, and I is the moment of inertia of the nitroxide ring about the C—N bond. This has the solution

$$\theta = \Theta \sin(2\pi\nu t)$$

where

$$\Theta = (kT/E_A)^{1/2} \qquad \nu = (E_A/2\pi^2 I)^{1/2} \qquad \text{(A2)}$$

Θ is the angular amplitude of oscillation and ν is the oscillation frequency. Using appropriate values for E_A (Gelin & Karplus, 1975) and I gives $\nu \sim 10^{-12}$ s^{-1}. This frequency is in the rapid motion EPR time scale and will result in averaging of the nitroxide magnetic parameters over the solid angle Θ.

It should be noted that the parameter E_A is highly dependent on the assumed shape of the torsional potential. For example, if instead of the form in eq A1 one assumed a potential of the form $U = E_A(1 - |\cos\theta|)$, we would find $\Theta = (2kT/E_A)^{1/2}$, which differs from (A2) by a factor of $2^{1/2}$.

Furthermore, the orientation of the N–O· bond appears to be fairly flexible with respect to the C–N–C plane of the nitroxide ring (Davis et al., 1975). Thus, small amplitude fluctuations of the N–O· bond orientation are also plausible and would produce spectral effects equivalent to torsional oscillation of the ring. Thus the torsional barrier parameter, E_A, is probably best considered as simply describing the mean amplitude of angular fluctuation, Θ.

The resonance positions of the hyperfine lines depend on the orientation of the nitroxide principal axes with respect to the magnetic field, with the outer lines in the "powder spectrum" arising primarily from nitroxides whose principal z axis is parallel to the magnetic field (McConnell & Gaffney-McFarland, 1970). For a nitroxide with the principal axis oriented at an arbitrary angle, ψ, with respect to the magnetic field, the effective hyperfine splitting, $2A(\psi)$, is given by

$$2A(\psi) = 2(A_{zz}^2 \cos^2\psi + A_\perp^2 \sin^2\psi)^{1/2} \qquad \text{(A3)}$$

where the hyperfine tensor is assumed to have axial symmetry ($A_{xx} = A_{yy} = A_\perp$) and A_{zz} and $A_\perp$ are the z and axial components, respectively. For small angles this can be expanded as

$$2A(\psi) = 2A_{zz}\cos\psi \times (1 + \tfrac{1}{2}(A_\perp^2/A_z^2)\tan^2\psi - \tfrac{1}{8}(A_\perp^4/A_z^4)\tan^4\psi \ldots)$$

For orientations near that of the magnetic field, i.e., near $\psi = 0$, only the first-order term will contribute and

$$2A(\psi) \simeq 2A_{zz}\cos\psi \qquad \text{(A4)}$$

With the assumption that $A_{zz} \simeq 34$ G and $A_\perp \simeq 6.5$ G (McCalley et al., 1972), this approximation will produce less than 2% error for angles $\psi \leq \pi/4$.

The effect of rapid torsional oscillation on the outer hyperfine lines, then, will be to average the hyperfine separation over the solid angle Θ centered around the magnetic field direction, or

$$2A_{obsd} = \frac{\int d\Omega[2A(\psi)]}{\int d\Omega} = \frac{2A_{zz}\int_0^\Theta (\cos\psi)(\sin\psi)\,d\psi}{\int_0^\Theta (\sin\psi)\,d\psi}$$

giving

$$2A_{obsd} = A_{zz}(1 + \cos\Theta) \qquad \text{(A5)}$$

Substituting in the expression for Θ derived above (eq A2), we find then that torsional oscillation will give us a temperature-dependent hyperfine separation of the form

$$2A_{zz}(T) = A_{zz}^0[1 + \cos[(kT/E_A)^{1/2}]] \qquad \text{(A6)}$$

where $2A_{zz}^0$ is the hyperfine separation in the absence of any motion.

Conformational Transitions. Conformational transitions of the nitroxide ring might be another mechanism which could give rise to a temperature-dependent hyperfine separation in some systems. A thermally activated inversion of the N–O· bond about the C–N–C plane, for example, would produce a temperature-dependent averaging of the inversion angle. However, from a review of reported nitroxide crystal structures, it appears that only six-membered rings in the chair form have N–O· bonds which are not planar with the C–N–C plane (Lajzerowicz-Bonneteau, 1976). Likewise, data from EPR crystallographic studies of Mal-6-labeled horse Hb suggest that the Mal-6 nitroxide ring probably exhibits only one ring conformation within its binding site (although more than one label binding orientation may be possible) (Chien, 1979). Thus it appears unlikely that ring conformational transitions contribute significantly to the temperature behavior observed here.

References

Abraham, E. C., Walker, D., Gravely, M., & Huisman, T. H. J. (1975) *Biochem. Med. 13*, 56–77.

Alpert, S. S., & Banks, G. (1976) *Biophys. Chem. 4*, 287–296.

Antonini, E., & Brunori, M. (1971) in *Hemoglobin and Myoglobin in Their Reactions with Ligands*, North-Holland Publishing Co., Amsterdam.

Barr, A. J., Goodnight, J. H., Sall, J. P., & Helwig, J. T. (1976) *A User's Guide to SAS 76*, Sparks Press, Raleigh, NC.

Bolton, J. R., Borg, D. C., & Swartz, H. M. (1972) in *Biological Applications of Electron Spin Resonance* (Swartz, H. M., Bolton, J. R., & Borg, D. C., Eds.) pp 63–118, Wiley-Interscience, New York.

Brown, D. G., Maier, T., & Drago, R. S. (1971) *Inorg. Chem. 10*, 2804–2806.

Chien, J. C. W. (1979) *J. Mol. Biol. 133*, 385–398.

Cohen, A. H., & Hoffman, B. M. (1973) *J. Am. Chem. Soc. 95*, 2061–2062.

Davis, T. D., Christofferson, R. E., & Maggiora, G. M. (1975) *J. Am. Chem. Soc. 97*, 1347–1354.

Gelin, B. R., & Karplus, M. (1975) *Proc. Natl. Acad. Sci. U.S.A. 72*, 2002–2006.

Goldman, S. A., Bruno, G. V., & Freed, J. H. (1972) *J. Phys. Chem. 76*, 1858–1860.

Griffith, O. H., Dehlinger, P. J., & Van, S. P. (1974) *J. Membr. Biol. 15*, 159–192.

Humphries, G. M. K., & McConnell, H. M. (1976) *Biophys. J. 16*, 275–277.

Hwang, J. S., Mason, R. P., Hwang, L.-P., & Freed, J. H. (1975) *J. Phys. Chem. 79*, 489-511.
Hyde, J. S., & Thomas, D. D. (1973) *Ann. N.Y. Acad. Sci. 222*, 680-692.
Hyde, J. S., Smigel, M. D., Dalton, L. R., & Dalton, L. A. (1975) *J. Chem. Phys. 62*, 1655-1677.
Johnson, M. E. (1978) *Biochemistry 17*, 1123-1228.
Johnson, M. E. (1979a) *FEBS Lett. 97*, 363-366.
Johnson, M. E. (1979b) *Biochemistry 18*, 378-384.
Jones, C. R., Johnson, C. S., & Penniston, J. T. (1978) *Biopolymers 17*, 1581-1593.
Kabankin, A. S., Zhidomirov, G. M., & Buchachenko, A. L. (1973) *J. Magn. Reson. 9*, 199-204.
Kang, S. Y., Gutowsky, H. S., Hsung, J. C., Jacobs, R., King, T. E., Rice, D., & Oldfield, E. (1979) *Biochemistry 18*, 3257-3267.
Lajzerowicz-Bonneteau, J. (1976) in *Spin Labeling: Theory and Applications* (Berliner, L. J., Ed.) pp 239-249, Academic Press, New York.
Lim, Y. Y., & Drago, R. S. (1971) *J. Am. Chem. Soc. 93*, 891-894.
Lozos, G. P., & Hoffman, B. M. (1974) *J. Phys. Chem. 78*, 2110-2116.
Mailer, C., & Hoffman, B. M. (1976) *J. Phys. Chem. 80*, 842-846.
McCalley, R. C., Shimshick, E. J., & McConnell, H. M. (1972) *Chem. Phys. Lett. 13*, 115-119.
McConnell, H. M., & Gaffney-McFarland, B. (1970) *Q. Rev. Biophys. 3*, 91-136.
Morishima, I., Kazunaka, E., & Yonezawa, T. (1973) *J. Chem. Phys. 58*, 3146-3154.
Murata, Y., & Mataga, N. (1971) *Bull. Chem. Soc. Jpn. 44*, 354-360.
Stone, T. J., Buckman, T., Nordio, P. L., & McConnell, H. M. (1965) *Proc. Natl. Acad. Sci. U.S.A. 54*, 1010-1017.
Thomas, D. D., Dalton, L. R., & Hyde, J. S. (1976) *J. Chem. Phys. 65*, 3006-3024.

Lanthanide Ion Luminescence Probes. Characterization of Metal Ion Binding Sites and Intermetal Energy Transfer Distance Measurements in Calcium-Binding Proteins. 1. Parvalbumin†

Moo-Jhong Rhee, Daniel R. Sudnick, Valerie K. Arkle, and William DeW. Horrocks, Jr.*

ABSTRACT: Eu(III) laser excitation spectroscopy of the $^7F_0 \rightarrow {}^5D_0$ transition reveals spectral features characteristic of the occupation of the CD and EF Ca(II)-binding sites of parvalbumin by Eu(III) ions. In addition, at pH 6.5, a signal attributable to binding at a third site is observed. This feature is abolished upon lowering the pH to 3.8. At pH 6.5, the appearance of this feature correlates with the decrease in luminescence intensity during titrations of parvalbumin with Eu(III) or Tb(III) after more than ~1.8 equiv of either of these ions has been added. Eu(III) ions in the primary sites coordinate zero to two H_2O molecules while the third site involves about three coordinated H_2O molecules. Parvalbumins in which mixed pairs of lanthanide ions, Ln(III), occupy the CD and EF sites were prepared. Nonradiative energy transfer between Eu(III) and Tb(III) acting as luminescent donors and various other Ln(III) ions serving as acceptors was observed by monitoring the excited-state lifetimes of the donor ions using a pulsed dye laser apparatus. With the assumption of a Förster-type dipole–dipole mechanism, inter-binding-site distance estimates were made from our measurements and are in reasonable agreement with the distance (11.8 Å) obtained by X-ray crystallography, especially when Eu(III) is the donor. R_0 values (critical distances for 50% energy transfer) in H_2O solution range from 9.2 Å for the Tb(III)–Ho(III) donor–acceptor pair down to 5.7 Å for the Eu(III)–Ho(III) pair.

The use of trivalent lanthanide ions, Ln(III), as metal ion replacement probes in calcium-binding proteins is well established (Reuben, 1979; Ellis, 1977; Nieboer, 1975). The ability of certain Ln(III) ions, notably Tb(III) and Eu(III), to serve as luminescence probes has been noted (Horrocks & Sudnick, 1979a,b; Martin & Richardson, 1979). Of particular interest is the use of Tb(III) to Co(II) or Fe(III) Förster-type (Förster, 1948, 1965) energy transfer to measure distances between metal ion binding sites in proteins (Horrocks et al., 1975; Berner et al., 1975; Meares & Ledbetter, 1977). In this and the following paper (Snyder et al., 1981) we seek to establish inter-Ln(III)-ion energy transfer as a distance probe for use in calcium-binding proteins. Since there are a large number of proteins with two or more calcium-binding sites (Kretsinger, 1976; Kretsinger & Nelson, 1976), this class of probe holds the promise of considerable utility. The object of study in the present paper is a particular parvalbumin isotype from carp muscle (carp-III, pI = 4.25). Its primary sequence is known (Coffee & Bradshaw, 1973), and its complete three-dimensional X-ray structure has been determined to 1.85 Å resolution (Kretsinger & Nockolds, 1973). Furthermore, the coordination of Tb(III) to the two calcium-binding sites, denoted CD and EF, has been studied by X-ray techniques (Sowadsky et al., 1978). Parvalbumin thus provides a well-characterized model system on which to study inter-Ln(III)-ion energy transfer between the CD and EF sites which are separated by 11.8 Å in the native protein. In addition, using the Eu(III) ion excitation spectroscopic technique introduced by us earlier (Horrocks & Sudnick, 1979b), we are able to establish the details of Ln(III) ion binding to parvalbumin including the characterization of a third binding site.

† From the Department of Chemistry, The Pennsylvania State University, University Park, Pennsylvania 16802. *Received July 24, 1980; revised manuscript received January 22, 1981.* Supported by Grant GM-23599 from the National Institute of General Medical Sciences, National Institutes of Health. Matching funds for the purchase of the departmental Mod-Comp computer and laser facilities were provided by the National Science Foundation.

0006-2960/81/0420-3328$01.25/0